Journal of Alloys and Compounds 513 (2012) 294–299

Contents lists available at SciVerse ScienceDirect

Journal of Alloys and Compounds

journal homepage: www.elsevier.com/locate/jallcom

First principles studies of band structure and electronic properties of ZnSe

B.I. Adetunji [a], P.O. Adebambo [a], G.A. Adebayo [a,b,*]

[a] Department of Physics, University of Agriculture, PMB 2240, Abeokuta, Nigeria
[b] The Abdus Salam International Centre for Theoretical Physics, Strada Costiera 11, I-34014 Trieste, Italy

ARTICLE INFO

Article history:
Received 20 August 2011
Received in revised form 7 October 2011
Accepted 10 October 2011
Available online 21 October 2011

Keywords:
Electronic properties
Band structure
First-principles calculations
Density functional theory
Local density approximation
Generalized gradient approximation

ABSTRACT

The structural and electronic properties of semiconductor ZnSe are investigated by performing first principles calculations using density functional theory (DFT). The exchange correlation potentials were treated within the local density approximation (LDA) and the generalized gradient approximation (GGA) with the quantum espresso package. We calculate the density of state (DOS), projected density of state (PDOS), phonon dispersion frequencies and the electron charge density. Also, the bulk modulus and its pressure derivatives are determined. Where available, the calculated quantities are compared with known results. The electronic band structure revealed an occurrence of a 2.72 eV band gap, while the density of state shows split peak at −2 eV and a minor peak split between 8 and 11 eV. We show that from the gamma points, along the high symmetries $\Gamma \rightarrow X$ and $\Gamma \rightarrow L$ directions, there are four dispersion (OL, OT, AL and AT) mode curves which later split into six modes along the $X \rightarrow \Gamma$ (2OL, OT, 2AT, and AL), $L \rightarrow X$ (2OT, OL, 2AT, and AL), $X \rightarrow W$ (2OL, OT, 2AT, and AL) and $W \rightarrow L$ (2OT, OL, 2AT, and AL) directions. These modes splitting correspond to optical longitudinal mode, optical transverse mode, acoustic longitudinal mode and acoustic transverse mode.

1. Introduction

The technological importance of groups II–VI semiconductor compounds and their alloys have attracted more and more attention is recent time; especially due to their applicability, they found applications in optoelectronic devices and detectors [1–5]. ZnSe (zincblende) is a II–VI semiconductor compound with a band gap of 2.70 eV [6]. Hence, it has played a prominent role in optoelectronic devices specifically, in the blue green region of the electromagnetic spectrum [7–11]. The electronic, transport and magnetic properties of the semiconductor compound have generated more interest in recent time due to the application of the compound in sprintonic [1]. Therefore, a large number of investigations and calculations of the optical properties, structural and band structure had been performed. In the work of Walter and Cohen, the reflectivity spectrum and valence charge density of ZnSe was reported along other semiconductor compounds [12,13]. The empirical pseudopotential method was used by Chelikowsky et al. [14] to study the valence band density of states (DOS) of zincblende semiconductors and diamond. The structural and electronic properties of the binary semiconductor compounds including ZnSe were investigated by Rabah et al. [15] using FP-LAPW within the local spin density approximation. The electronic properties of ZnX (X = S, Se, Te) were reported by Khenata et al. [16] using the full-potential linear augmented plane-wave method plus local orbitals. Also, the tight binding linear muffin–tin orbital (TB-LMTO) method was applied by Gangadharan et al. [17] to investigate the electronic properties of ZnX semiconductor compounds. Rodriguez et al. [18] used tight binding scheme to calculate electronic projected bulk band structure, surface band structure and the wave vector resolved density of states for II–VI semiconductors, while Cui et al. [19] studied the energy–volume curves of all the phases of ZnSe using the PP–PW method. Although, one can find in literature, the various work done on the electronic structure and band calculations of ZnSe, to the best of knowledge, this is the first time an attempt has been made to classify the mode splitting that occurred in this semiconductor alloy.

The purpose of this work is to present the ground state properties such as equilibrium lattice parameter, static bulk modulus (B), first order pressure derivative of the bulk modulus (B'), electronic structure, density of state, projected density of state and the phonon dispersion frequency mode splitting of ZnSe semiconductor compound using density functional theory as implemented in the quantum espresso package.

* Corresponding author at: Department of Physics, University of Agriculture, PMB 2240, Abeokuta, Nigeria.
E-mail addresses: gadebayo@ictp.it, Adebayo@physics.unaab.edu.ng (G.A. Adebayo).

0925-8388/$ – see front matter © 2011 Elsevier B.V. All rights reserved.
doi:10.1016/j.jallcom.2011.10.039

2. Theory and computational procedure

2.1. Total energy and functional

Solving the many-body Schrödinger equation allows to obtained many properties of a system of N interacting electrons in the external potential of the nuclei. The Hamiltonian equation is given as:

$$H_\psi(r_1, \ldots, r_{Nel}) = E_\psi(r_1, \ldots, r_{Nel}) \quad (2.1.1)$$

while the Schrödinger equation is stated below:

$$H = -\sum_i \frac{\hbar^2}{2M\Delta_i^2} + \sum_i V_{ext}(r_i) + \frac{e^2}{2}\sum_{i\neq j}\frac{1}{|r_i - r_j|} \quad (2.1.2)$$

where r_i is the position of electron i, Δ_i^2 indicates the Laplacian taken with respect to the coordinate r_i, while $V_{ext}(r_i)$ is the external potential acting on the electrons and depends parametrically on the nuclear positions. In finding a numerical solution for the Schrödinger Eq. (2.1.1), an efficient method is required. Density functional theory (DFT) introduced by Hohenberg and Kohn [20] provides a one-to-one correspondence between the ground-state electronic charge density $\rho(r)$ and the external potential $V_{ext}(r)$. Therefore, since the external potential determines also the many-body wave-function of the ground state, every physical quantity of the system in its ground state can be expressed as a functional of the electronic charge density. The ground-state total energy of the system plays a prominent role in determining properties of a system, this can be expressed as the expectation value of the Hamiltonian on the ground-state wave-function Ψ_0. If we express the total energy as a functional of the electronic density then [20,21],

$$E[\rho(r)] = \langle\Psi_0|H|\Psi_0\rangle = F[\rho(r)] + \int_v V_{ext}(r)\rho(r)d^3r \quad (2.1.3)$$

where the integral is performed over the whole volume V of the system. In this Eq. (2.1.3), $F[\rho(r)]$ is a universal functional of the density and it is given by the expectation value of the kinetic energy and of electrostatic electron repulsion terms on the ground state. The minimization of the functional $E[\rho(r)]$ with respect to the electronic density, with the constraint that the number of electrons N_{el} is fixed,

$$\int_v \rho(r)d^3r = N_{el} \quad (2.1.4)$$

gives the ground-state total energy and the electronic density. Kohn and Sham (KS) [21] introduced a new functional by mapping the many-body problem into a non-interacting electrons problem with the same ground-state electronic density because, the exact form of the universal functional $F[\rho(r)]$ is not known. The new functional can be obtained by recasting the second term in Eq. (2.1.3) to the form [20,21]:

$$F[\rho(r)] = T_0[\rho(r)] + E_H + E_{xc}[\rho(r)] \quad (2.1.5)$$

where the first term is the kinetic energy of a non-interacting electrons system, the second term is the Hartree-like energy term, which accounts for the classical Coulomb interaction of a spatial charge distribution $\rho(r)$ and the third term represents the exchange-correlation energy [20,21]. The only really unknown quantity is the exchange-correlation energy functional and, in principle, the quality of the solution of the full many-body problem will be only limited by the quality of the approximation. With this new expression for the functional then, the total energy in Eq. (2.1.3) becomes:

$$E[\rho(r)] = \langle\Psi_0|H|\Psi_0\rangle = T_0[\rho(r)] + E_H + E_{xc}[\rho(r)] + \int_v V_{ext}(r)\rho(r)d^3r \quad (2.1.6)$$

In order to account for the exchange-correlation energy functional in the above equation, we applied a local density approximation (LDA) and generalized gradient approximation (GGA) [20,21].

2.2. Equation of state and elastic properties

The thermodynamic equation that described and explained state of matter under specified physical conditions is known as equation of state. The equations of state consist of mathematical relationship between two or more state functions such as temperature, pressure and volume. In order to determine the energy–volume relationship which allows us to obtain the equilibrium lattice parameter, we adopt the method proposed by Birch–Murnaghan [22] to fit the data generated by energy–volume calculations;

$$\Delta E(V) = E - E_0 = BV_0\left[\left(\frac{V_n}{B'}\right) + \left(\frac{1}{1-B'}\right) + \left(\frac{V_n}{B'(B'-1)}\right)\right] \quad (2.2.1)$$

where V_0 is the equilibrium volume at zero pressure, E_0 is the equilibrium energy and B, B' are the bulk modulus and its derivative. Taking the derivative of Eq. (2.2.1) we compute the bulk modulus and subsequently obtained the derivative of the bulk modulus.

2.3. Density of state

By solving the KS equation for a system at different values of wave vector $\mathbf{k}$, one can obtained the dispersion relation ($\mathbf{k}$, ϵ_{kv}) which makes it possible to compute the density of state (DOS)

$$\rho(E) = \sum \delta(E - \epsilon_{kv}) \quad (2.3.1)$$

which is defined here as a sum of Dirac delta functions centred at energy values corresponding to the eigenvalues of the KS equation. In practice this summation is performed by substituting $\delta(\epsilon)$ with a regular and continuous function $\delta(\epsilon)$ which has the same normalization as $\delta(\epsilon)$. In this work we used Gaussian functions with a spread controlled by a smearing parameter t as given below:

$$\delta(\epsilon) = \left(\frac{1}{\sqrt{2\pi}t}\right)\exp -\left(\frac{\epsilon}{2t}\right)^2 \quad (2.3.2)$$

In order to reach a good approximation of the exact limit of the DOS given in Eq. (2.3.2) and corresponding to the limit $t \to 0$, a small value of the smearing has to be chosen. However, since the number of k points needed to converge the DOS increases very fast as t decreases, in practical calculations one makes a trade-off between the desired accuracy (essentially, how much fine structures can be resolved in the DOS) and the computational cost given by the number of k points.

2.4. Computational procedure

The theories of first-principles methods are well established [20–24] and have been applied in the studies of structural and electronic properties of materials [25–27]. The local density approximation (LDA) and generalized gradient approximation (GGA) are used in first-principles total energy calculations by using plane-wave self-consistent field (PWSCF) method as implemented in the quantum espresso package [28]. Core electrons are treated explicitly by employing Vanderbilt ultrasoft pseudopotential as supplied by Perdew–Zunger and non linear core correction [29–31,33]. The set of irreducible k-points used was generated by a Monkhorst–Pack scheme [34], while a plane-wave basis set with an energy cut-off of 30 Ry was applied.

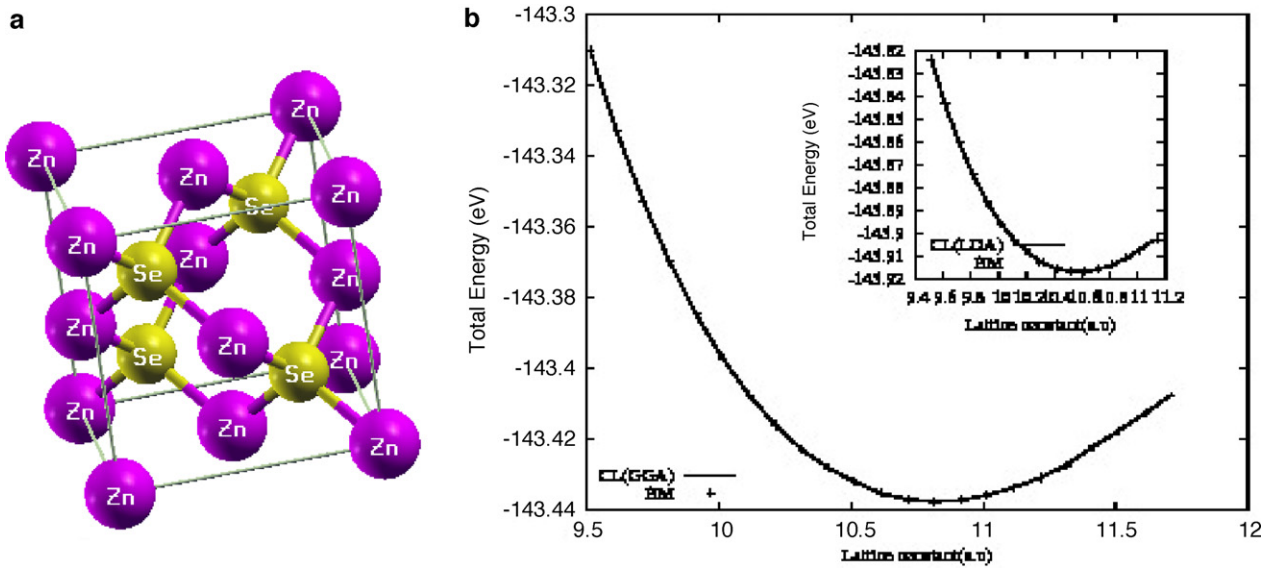

Fig. 1. (a) Crystal structure of ZnSe showing Zn atoms at the edges and on the six faces. The Se atom makes it possible to form two inter-penetrating face centred cubic lattices. (b) The total energy (eV) against calculated values of lattice parameter (a.u.), with both LDA and GGA. Inset is the LDA and Birch–Murnaghan (BM) fitted values.

Essentially, our calculations of the electronic band structure involve, a single point self-consistent calculation after which non self-consistent $4 \times 4 \times 4$ uniform grid calculations are performed. However, in the calculations of the density of states, the occupancy of the bands is determined using tetrahedra method with an automatic and uniform k-point generations. A two step procedure [28] was employed in the phonon frequencies calculations by finding the ground state (both atomic and electronic) configurations and subsequently using the density functional perturbation theory. In order to get a well converged ground state energy, the Brillouin Zone was sampled with $4 \times 4 \times 4$ k-points mesh and to test the accuracy of the plane-wave basis set and that of the Vanderbilt ultrasoft pseudopotential, we determined the equilibrium lattice parameter, bulk modulus and the pressure derivatives of the bulk modulus of ZnSe by the standard procedure for computing the total energy for different lattice constant and fitted these to Murnaghan's equation of states [22,28].

3. Results and discussion

3.1. Structures of zincblende

Structurally, zincblende occurs in different cubic phases and in particular, ZnSe is face centred with space group F43m. The cubic symmetry of ZnSe is such that the Zn atoms occupy the edges and faces positions while the Se atoms allow the crystal to form inter-penetrating face centred cubic. The structure therefore looks like a two-component diamond structure with no symmetry inversion (Fig. 1a). In our calculations, we perform an optimization of the lattice parameter by energy minimization; different values of lattice constants are used to generate corresponding total energy values within a given energy cut-off value (30 Ry) The obtained total energies and lattice constants data are then fitted to the Birch–Murnaghan equation of state [22]. Fig. 1b shows agreement between the present calculations and other reported values [19], but with 1.3 and 1.06% deviation from the experimental result of Ref. [35] respectively in the cases of LDA and GGA, while in Table 1, we compared our calculated equilibrium lattice parameter, bulk modulus (B) and the pressure derivative of bulk modulus (B') with other reported work [19,35–37]. The deviation in the lattice parameter with experimental value is typical of first principles calculations using LDA and GGA approximations, usually, the calculated band gap is much smaller than the experimentally determined one. Therefore, a correction to the LDA was performed using quasiparticle energies as reported in [40]. The calculated bulk modulus (B) and its pressure derivative are in good agreement with other results found in the literature (as shown in Table 1). There are about 4.85 and 10.5% deviations from experimental result [35] with both LDA and GGA. This trend is also observed in the pressure derivative of the bulk modulus (B').

3.2. The electronic structure

Electronic structure at the ground state provides among other things, an important way of understanding the behavior of materials at microscopic level. The (GGA) band structure of ZnSe including the low-lying states along the high-symmetry points of the BZ is shown in Fig. 3a, for clarity, the Fermi level has been set to zero. Clearly, the calculated band gap is 2.72 eV; this is in agreement, within acceptable error, with other results [19,35].

The charge density is a ground state property of a crystal which is important for an understanding of the structure and chemical bond in crystalline materials. It is also a complementary way of understanding the electronic structure of crystals. The calculated charge density distribution is shown in Fig. 2, this gives visual nature of

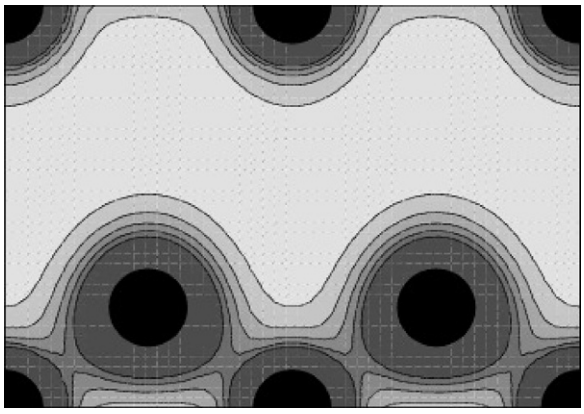

Fig. 2. The charge density of ZnSe.

Table 1
Lattice constant (a), bulk modulus (B) and pressure derivative of bulk modulus (B') of ZnSe at 0 GPa and 0 K.

Material	Parameter	Present results	Other calculated results	Experimental value
ZnSe	a (a.u.)	5.594[e], 5.728[f]	5.578[a], 5.820[b], 5.669[c]	5.667[d]
	B (GPa)	68.00[e], 58.50[f]	71.84[a], 52.92[b], 67.6[c]	64.7[d]
	B'	4.07[e], 3.94[f]	4.599[a], 3.81[b], 4.67[c]	4.77[d]

[a] From the FP-LAPW method [36].
[b] From the NAO + GC method [37].
[c] From the PP–PW method [19].
[d] Ref. [35].
[e] LDA.
[f] GGA results.

chemical bonds found in ZnSe. The result shows spherical charge densities around the Zinc ions, but a small bond charge inside the selenium ion which is an effect of hybridization due to charge sharing by Zinc and Selenium sp orbital.

From the band structure (Fig. 3a), the difference between the valence band and the conduction band levels is very small (in terms of energy difference i.e. there are few eV band gaps), this is an indication that ZnSe possesses semiconductor properties. This same trend is observed from the density of state (DOS) (Fig. 3b). A direct band gap is noticed in the band structure of Fig. 3a. The total projected density of state (PDOS) is presented in Fig. 3c along with the total density of state (DOS). The projected density of state gives a clearer picture of the elemental contributions to the electronic structure of ZnSe. From Fig. 3b and c, the structures in the DOS are located in the energy range −4 and 14 eV, with a dominant structure having a split peak appearing at −2 eV and a minor peak split between 8 and 11 eV (in Fig. 3b). We expect the split in this region to correspond to a spin–orbit split with a value corresponding to the energy value between two transitions [38]. In addition, inset (Fig. 3b) is transitions in the energy range 5 and 14 eV with lightly populated energy states. The projected density of state (PDOS) is computed based on the dispersion relation and the pseudo-wavefunctions of the eigenstates of the KS equation. PDOS is the density of state projected onto the atomic wavefunction, it

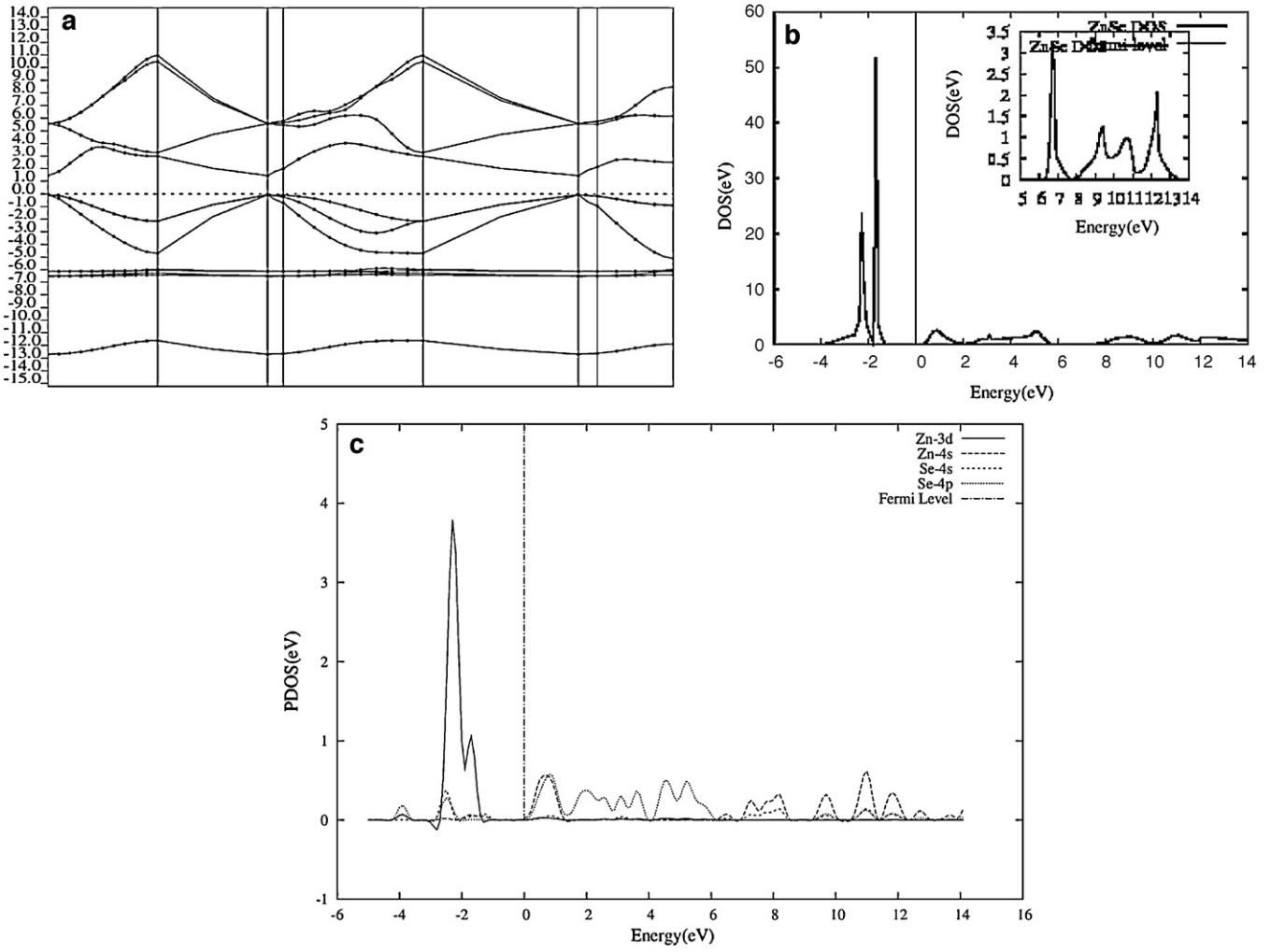

Fig. 3. (a) The high symmetry directions are from left to right K, W, X, G, L, W, X, G. (b) The density of state for ZnSe. Inset shows the density of state within the energy range of (5–14 eV). The Fermi level is located on the vertical line at point zero on the x-axis. (c) The projected density of state of ZnSe, the Fermi level has been shifted to zero on the x-axis.

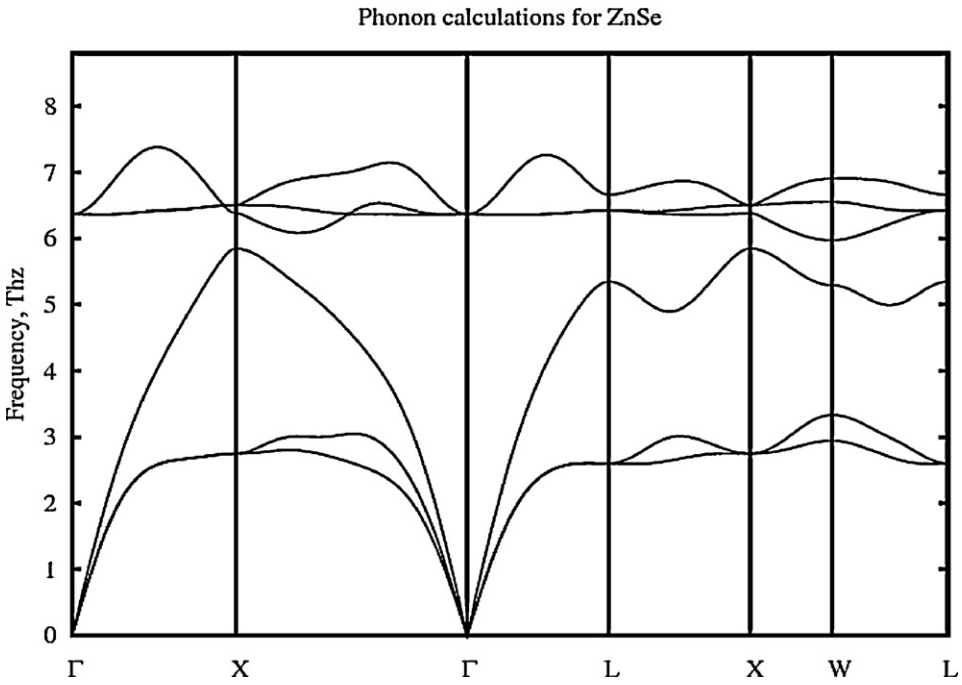

Fig. 4. phonon dispersion frequencies along high-symmetry Brillouin Zone.

gives a clearer picture of the elemental contributions to the electronic structure as shown in Fig. 3c. At around −4 eV, pre-peaks are noticed in the Zn-3d, Zn-4s and Se-4p orbitals with the 4p orbitals having higher PDOS value, between −3 and −2 eV, only the Se-4s and Se-4p orbitals have pre-peaks. However, in this energy range, the Zn-3d has a depression of magnitude 0.00944 eV. At −2 eV, a split peak is seen in the Zn-3d orbital. The peaks between the Fermi level and 14 eV (Fermi level is shifted to zero) are due to the Zn-4s and Se-4p orbitals. Hence, due to hybridization, both Zn-4s and Se-4p states contribute more to conduction band as shown in Fig. 3c.

3.3. *Phonon frequency*

Phonon study is important in solid state physics and materials science because, it gives a clear understanding of the physical properties of materials such as the thermal expansion coefficients, electrical conductivities, Debye temperature, specific heat, electron–phonon interactions, etc. The frequency of vibration is a function of wave vector **k**, which can be written with the dispersion relation as $\omega(\mathbf{k}) = \Sigma\omega_j(k)$. In the zincblende ZnSe crystal lattice, there are two atoms per unit cell, which resulted into six branches of dispersion curves. Due to translational symmetry, $\omega_j(\mathbf{k}+\mathrm{G}) = \omega_j(k)$ then, only phonon frequencies in the first Brillouin Zone can be calculated. Along some high symmetry points, we are able to calculate the phonon dispersion curves for ZnSe as shown in Fig. 4. Our calculation is in good agreement with for example Ref. [32]. The present calculations show that from the gamma points, along the high symmetries $\Gamma \rightarrow$ X and $\Gamma \rightarrow$ L directions, there are four branches of dispersion curves which later split into six branches along the X → L, L → X and X → W directions.

By differentiating the phonon frequencies into four modes via acoustic longitudinal mode (AL), acoustic transverse mode (AT), optical longitudinal mode (OL) and optical transverse mode (OT) at the BZ boundary, it is possible to characterize the high symmetry directions and identify which split corresponds to any of the modes. In the optical branch, identifying the transverse mode or longitudinal mode is difficult except one put into consideration the mass ratio of the constituent atoms and their ionicity [38]. On the other hand, in the acoustic branch such difficulty does not exist because, the transverse frequency is smaller than the longitudinal frequency except at zone centres where both modes have zero frequency. The argument put forward by Mitra in Ref. [38] will be very helpful to classify the splits: In elemental crystals, the optical branch degenerate at the zone centres with the transverse optical phonon having higher energies than the longitudinal modes at or near the zone boundary. For compounds with low ionicity at the zone centre, the OL mode has higher frequency than the OT mode while near the zone boundary, the OT is at higher frequency than the OL mode [38,39].

From Fig. 4 and using the above notations, we see that in the directions $\Gamma \rightarrow$ X and $\Gamma \rightarrow$ L the optical and acoustic branches both split into transverse and longitudinal modes while in the X → Γ, L → X, X → W and W → L directions there are "mode splitting. "Furthermore, the curve above 7 THz is an OL mode while the curve above 6 THz is an OT mode. Similarly, the curve above 2.5 THz is an AT mode while the curve above 5 THz is an AL mode. In the "mode splitting" regimes, the AT mode splits into two separate AT modes leading to 2AT + 1AL (3 modes). The optical branch is characterized by splitting of both the OL and OT modes in these regimes. For example, in the regime X → Γ, there are 2OL + 1OT (3 modes), in the regime L → X, there are 2OT + 1OL (3 modes), in the regime X → W, there are 2OL + 1OT (3 modes) and lastly, in the W → L regime, there are 2OT + 1OL (3 modes).

4. Conclusions

In summary, we have calculated by first-principles ab initio method, the electronic lattice parameter, charge density, band structure, density of state and projected density of state of ZnSe. Our calculated optimized lattice parameters of 5.594 (LDA) and 5.728 (GGA) a.u. is in close agreement with experimental and other calculated results available for this system. The calculated structural properties are in good agreement with available results. Also, this work revealed that ZnSe has direct band gap of 2.72 eV. Furthermore, we have reported the calculation of phonon dispersion

frequency for ZnSe using linear response theory method, making it possible for us to characterize the entire mode splitting either into four or six dispersion modes. And lastly, this work revealed the type of mode splitting present in ZnSe.

Acknowledgments

The authors (BIA and POA) are grateful to the Marie Curie Library of the Abdus Salam International Centre for Theoretical Physics (ICTP) for permission to use the eJDS facility for reference searching. One of us, GA acknowledges financial support and hospitality from the (ICTP) as Regular Associate.

References

[1] P.F. Peterson, et al., Phys. Rev. B 63 (2001) 165211.
[2] Y.Q. Li, et al., Appl. Phys. Lett. 88 (2006) 013115, doi:10.1063/1.2161073.
[3] Y. Pan, et al., J. Phys.: Condens. Matter 14 (2002) 10487, doi:10.1088/0953-8984/14/44/320.
[4] M. Côté, O. Zakharov, A. Rubio, M.L. Cohen, Phys. Rev. B 55 (1997) 13025.
[5] Tan Jia-Jin, et al., Commun. Theor. Phys. 53 (2010) 1160.
[6] G. Grebe, G. Roussos, H.-J. Schulz, J. Phys. C: Solid State Phys. 9 (1976) 4511–4516, doi:10.1088/0022-3719/9/24/020.
[7] T. Suski, Semicond. Semimet. 54 (1998) 485.
[8] S. Sanchez, et al., High Temp. Mater. Process 3 (1) (1999) 91.
[9] G. Neu, E. Tournié, C. Morhain, M. Teisseire, J.-P. Faurie, Phys. Rev. B 61 (2000) 15789.
[10] X. Wang, D. Huang, C. Sheng, G. Yu, J. Appl. Phys. 90 (2001) 6114, doi:10.1063/1.1415061.
[11] H. Pérez Ladrón de Guevara, et al., J. Phys. D: Appl. Phys. 35 (2002) 1408, doi:10.1088/0022-3727/35/12/318;
A.H. Reshak, S. Auluck, Physica B 388 (2007) 34.
[12] J.P. Walter, et al., Phys. Rev. B 1 (1970) 2661.
[13] J.P. Walter, M.L. Cohen, Phys. Rev. B 4 (1971) 1877.
[14] J. Chelikowsky, D.J. Chadi, L. Marvin, Cohen. Phys. Rev. B 8 (1973) 2786.
[15] M. Rabah, et al., Mater. Sci. Eng. B 100 (2003) 163.
[16] R. Khenata, et al., Comput. Mater. Sci. 38 (2006) 29.
[17] R. Gangadharan, et al., J. Alloys Compd. 359 (2003) 22.
[18] F. Rodriguez, A. Camachq, L. Quiroga, R. Baquero, Phys. Stat. Sol. (b) 160 (1990) 127.
[19] S.X. Cui, et al., J. Alloys Compd. 472 (2009) 294.
[20] P. Hohenberg, W. Kohn, Phys. Rev. B 136 (1964) 864.
[21] W. Kohn, L.J. Sham, Phys. Rev. 140 (1965) A1133.
[22] F.D. Murnaghan, Proc. Natl. Acad. Sci. U.S.A. 30 (1944) 244.
[23] R. Car, M. Parrinello, Phys. Rev. Lett. 55 (1985) 2471.
[24] R.M. Dreizler, E.K.U. Gross, Density Functional Theory, Springer-Verlag, Berlin, Heidelberg, 1990.
[25] G. Kresse, J. Furthmueller, Comput. Mat. Sci. 6 (1996) 15.
[26] W.R. Wadt, P.J. Hays, J. Chem. Phys. 82 (1985) 284, doi:10.1063/1.448800.
[27] R.M. Martin, Electronic Structure, Cambridge University Press, UK, 2004.
[28] P. Giannozzi, et al., J. Phys.: Condens. Matter 21 (2009) 395502.
[29] J.P. Perdew, A. Zunger, Phys. Rev. B 23 (1981) 5048.
[30] We used the pseudopotential Zn.pz-van_ak.UPF from www.quantum-espresso.org.
[31] We used the pseudopotential Se.pz-bhs.UPF from www.quantum-espresso.org.
[32] A.D. Corso, S. Baroni, R. Resta, Phys. Rev. B 47 (1993) 3588.
[33] D. Vanderbilt, Phys. Rev. B 41 (1990) 7892;
K. Laasonen, et al., Phys. Rev. B 43 (1991) 1696.
[34] H.J. Monkhorst, J.D. Pack, Phys. Rev. B 13 (1976) 5188.
[35] B.H. Lee, J. Appl. Phys. 41 (1970) 2988.
[36] J.E. Jaffe, R. Randey, M.J. Seel, Phys. Rev. B 47 (1993) 6299.
[37] V.I. Smelyansky, J.S. Tse, Phys. Rev. B 52 (1995) 4658.
[38] S.S. Mitra, Phys. Rev. 132 (1963) 986.
[39] R.W. Keyes, J. Chem. Phys. 37 (1962) 72.
[40] F. Roth, et al., New J. Phys. 12 (2010) 103036, doi:10.1088/1367-2630/12/10/103036, cited relevant references.